Methods for Benchmarking Photolithography Simulators: Part III

Mark D. Smith*, Trey Graves, Jeffrey D. Byers, Chris A. Mack
KLA-Tencor Corp.

ABSTRACT

In the past, most lithography simulators have used the thin-mask or Kirchhoff approximation to calculate the diffraction pattern for imaging calculations. This approximation has been very accurate for binary reticles, and rigorous solutions to the full Maxwell equations were only required for "exotic" technologies such as alternating phase-shift masks and chromeless phase lithography (CPL). For the future technology nodes, the thin-mask approximation may be insufficient even for binary reticles. This means that solution of the full Maxwell equations will be required for most, if not all, lithography simulations, and that these simulators must be robust and accurate, especially when used by someone who is not an expert in solving the Maxwell equations.

In a previous series of papers, we proposed benchmarks for lithography simulators drawn from the optics literature for aerial image and optical film-stack calculations. We extend this work and present benchmarks here for Maxwell equation solvers. These benchmarks can be easily applied to any mask topography simulator.

Keywords: Lithography simulation, numerical accuracy, PROLITH

1 INTRODUCTION

As numerical simulation becomes more important to the design and optimization of photolithographic processes, it becomes vital that simulators provide accurate results. A simulator must not only be accurate; it must become more accurate with each design node [1]. The driving force for greater accuracy from simulators is the same driving force demanding greater precision from metrology tools, where the P/T ratio (precision to tolerance) must remain the same as target CDs and tolerances shrink. For both simulators and metrology tools, a 5nm error might seem insignificant when engineering a 0.5 micron process, but it is a significant fraction of the error budget for a 65nm process.

Benchmarking the accuracy of a simulator should be an important part of an "acceptance test" for all simulation software. A P/T ratio of 0.1 to 0.2 is typical for metrology tools, so perhaps it would be reasonable for simulators as well. Benchmarking should be performed if you have purchased a commercial simulator (such as PROLITH) or if you are using a code that you or your colleagues have written for internal use at your company. Although it is obvious that software must be free of bugs or algorithm problems in order to make quantitative engineering decisions, few users of simulation software actually perform a quantitative study of the accuracy of their simulator.

One of the reasons relatively few quantitative accuracy studies are performed is that for the end-user of a simulator, it is often difficult to make a judgment regarding the accuracy of a simulator beyond whether a particular result is "reasonable". Of course, it is possible to compare one simulator with the results calculated with another simulator, but if the results do not agree, how do you decide which one is correct? In addition, both simulators could agree and still be incorrect. The approach taken in the current study is to find closed-form solutions from the research literature, and to use these solutions as an absolute standard for benchmarking lithography simulators. This is similar to the approach taken by Brunner [2] and Gordon [3].

The current work is an extension of our previous papers [4, 5], where we proposed standard benchmark problems for aerial image calculations and for image in resist calculations. The benchmarks presented here are for mask topography simulators which solve the Maxwell equations in order to determine the diffraction pattern. Benchmark problems for mask topography simulators are urgently needed because this type of calculation will likely be required for all lithography simulations for the 45nm node, and may be required for the 65nm node. This means that mask topography

* mark.d.smith@kla-tencor.com; phone 1-512-381-2318; 8834 North Capital of Texas Highway, Suite 301, Austin, TX 78759

Optical Microlithography XVIII, edited by Bruce W. Smith,
Proceedings of SPIE Vol. 5754 (SPIE, Bellingham, WA, 2005)
0277-786X/05/$15 · doi: 10.1117/12.601518

Downloaded From: http://proceedings.spiedigitallibrary.org/ on 05/06/2014 Terms of Use: http://spiedl.org/terms

simulators must be accurate, even when used by the non-expert who is unfamiliar with the idiosyncrasies of the numerical algorithms used to solve the Maxwell equations.

The outline of this paper is as follows: in Section 2, we review how a diffraction pattern is calculated from a mask by using the Maxwell equations, and we also outline some conventions, such as the choice of normalization for the diffraction order amplitudes. Next, we present benchmarks for mask blanks made up of planar film stacks in Section 3. This benchmark is relevant to transparent substrates coated with absorbing materials such as those used for chrome on glass mask blanks and for attenuated phase-shifting mask blanks. In Section 4, we examine simple grating structures formed by lossless materials. It is worthwhile to note that for this benchmark problem, we do require some elementary numerical methods – we must find the roots of a nonlinear algebraic equation, and then we must solve a linear algebra problem to find the reflected and transmitted diffraction orders. This is a departure from our previous work, where all of the benchmark tests were strictly in closed-form, and numerical methods were not required. However, for mask topography simulations, we felt that many of the closed-form problems were either almost trivial (such as the planar film stack problem in Section 3) or they were idealized systems that are difficult to set up with a simulator. One example of such an idealized system is the famous Sommerfeld half-plane problem. Here, a closed-form solution can be found for a plane wave incident on a semi-infinite, infinitely thin, perfect electrical conductor. Because all of the material and geometric attributes of this problem are mathematical idealizations that cannot be realized in a real photomask, it is difficult to determine if discrepancies between the closed-form solution and the numerical results are an error in the simulator or due to the fact that most mask topography simulators cannot simulate items that are infinitely thin or infinite in extent. For these reasons, we have neglected many of the elegant solutions that can be found in many electromagnetism texts in favor of the semi-analytic results presented for the dielectric grating problem in Section 4. Finally, our paper concludes with a summary and an outline future work in Section 5.

2 DEFINITION OF THE DIFFRACTION CALCULATION

One of the most important inputs to any optical lithography simulator is the model for the interaction between the illuminating electric field and the mask to form the diffraction pattern, see Figure 1. The diffraction pattern is then combined with a model for the objective lens of the stepper/scanner in order to predict the image at the wafer. Clearly, an error in the calculation of the diffraction pattern will lead to errors in the downstream results.

The thin-mask model (or Kirchhoff approximation) is the most common way to calculating the diffraction pattern. In this model, the transmittance of the mask is assumed to be ideal – different regions on the mask transmit the electric field with the ideal transmittance and phase, and the transition region between different types of features is a step function.

The more rigorous approach, solving the Maxwell equations, is the focus of the current work. There are many references on how to numerically solve the Maxwell equations and then extract the diffraction pattern from the results, so we will not go into the details here. However, one detail that is of critical importance when performing a quantitative benchmarking of Maxwell equation solvers is how the amplitudes in the diffraction pattern are normalized. In PROLITH, we chose a normalization that allows easy comparison of the Kirchhoff and Maxwell results. For the Kirchhoff result, the transmittance of an uncoated mask blank is unity, so we require that this condition be met for our mask topography simulator as well. This requirement can be easily satisfied after examination of the behavior of an incident plane wave at the planar boundary between two materials, as shown in Figure 2. If the incident field is given by $\boldsymbol{E}_I$ and the transmitted electric field $\boldsymbol{E}_T$, then the transmission coefficients are given by the Fresnel formulae, which depend on the polarization of the light and the angle of incidence, θ_1:

$$
\begin{aligned}
\tau_{12,s} &= \frac{E_{T,s}}{E_{I,s}} = \frac{2\mathbf{n}_1\cos(\theta_1)}{\mathbf{n}_1\cos(\theta_1)+\mathbf{n}_2\cos(\theta_2)} \\
\tau_{12,p} &= \frac{E_{T,p}}{E_{I,p}} = \frac{2\mathbf{n}_1\cos(\theta_1)}{\mathbf{n}_2\cos(\theta_1)+\mathbf{n}_1\cos(\theta_2)}
\end{aligned} \tag{1}
$$

Downloaded From: http://proceedings.spiedigitallibrary.org/ on 05/06/2014 Terms of Use: http://spiedl.org/terms

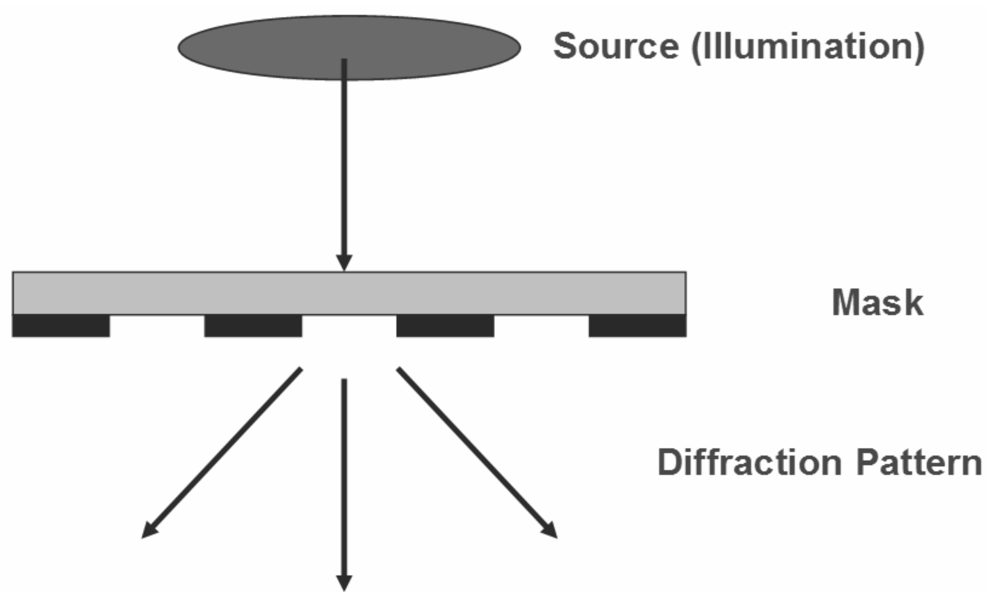

Figure 1: Interaction between the source illumination and the mask to form the diffraction pattern.

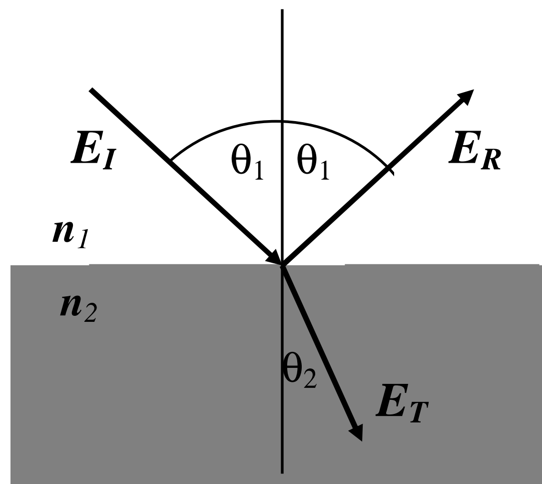

Figure 2: Diagram of the incident, transmitted, and reflected electric fields at an interface between two materials.

Downloaded From: http://proceedings.spiedigitallibrary.org/ on 05/06/2014 Terms of Use: http://spiedl.org/terms

The subscript s indicates the s-polarization, which is also called the TE (or transverse electric) polarization, where the electric field vector is perpendicular to the page in Figure 2. The subscript p indicates the p-polarization, which is also called the TM (or transverse magnetic) polarization, where the electric field vector lies within the page in Figure 2. The angle θ_2 can be found by Snell's law:

$$\mathbf{n}_1 \sin\theta_1 = \mathbf{n}_2 \sin\theta_2 \tag{2}$$

The normalization of the incident electric field for the diffraction calculation can be found by choosing a particular angle, setting $\boldsymbol{E}_T$ to a unit vector, and solving equations (1) for $\boldsymbol{E}_I$. For the normalization of the incident field amplitude, we choose the angle as zero, or the normally incident case:

$$E_I = \frac{n_{substrate} + 1}{2n_{substrate}} \tag{3}$$

where $n_{substrate}$ is the refractive index of the mask blank (usually quartz). In PROLITH, the refractive index of the mask blank is required to be real (non-absorbing) for transmissive masks. This normalization is used regardless of the actual incident angle at the mask. The reason for this is that if several diffraction patterns are calculated with a range of incident angles (for simulation of off-axis illumination) then a single normalization factor allows them to be re-combined in a consistent way.

3 TRANSMISSIVITY OF ABSORBING FILM STACKS

The first test is for a planar, absorbing film between two non-absorbing films, as shown in Figure 3. The transmissivity of this film stack is calculated as an example in the textbook by Born and Wolf, "An absorbing film on a transparent substrate", found in Section 13.4.1 of the 6th edition [6]. Although the solution of this problem is fairly straightforward, the resulting equations are algebraically complicated, so we will not present the solution here. Instead, we will present results for a specific test problem that is relevant to attenuated phase-shifted mask blanks. The interested reader can reproduce our results by using the equations in Born and Wolf.

The result of the solution by Born and Wolf is the transmissivity, while the quantity of interest is the amplitude of the electric field for the 0th transmitted diffraction order. We can convert the calculated transmissivity into the amplitude of the transmitted electric field as follows. First, the transmissivity is defined as the ratio of the transmitted irradiance to the incident irradiance:

$$T = \frac{J_T}{J_I} = \frac{\cos(\theta_T) I_T}{\cos(\theta_I) I_T} = \frac{n_T \cos(\theta_T)}{n_I \cos(\theta_I)} \left| \frac{E_T}{E_I} \right|^2$$

Where T is the transmissivity, J is the irradiance, and I is the intensity. As before, the subscripts I and T indicate the incident and transmitted quantities. Combination of the above definition with the normalization condition given by equation (3) gives the final result:

$$|E_T| = \sqrt{\frac{n_{substrate} \cos\theta_I}{\cos\theta_T} T} \; \frac{n_{substrate} + 1}{2n_{substrate}}$$

Downloaded From: http://proceedings.spiedigitallibrary.org/ on 05/06/2014 Terms of Use: http://spiedl.org/terms

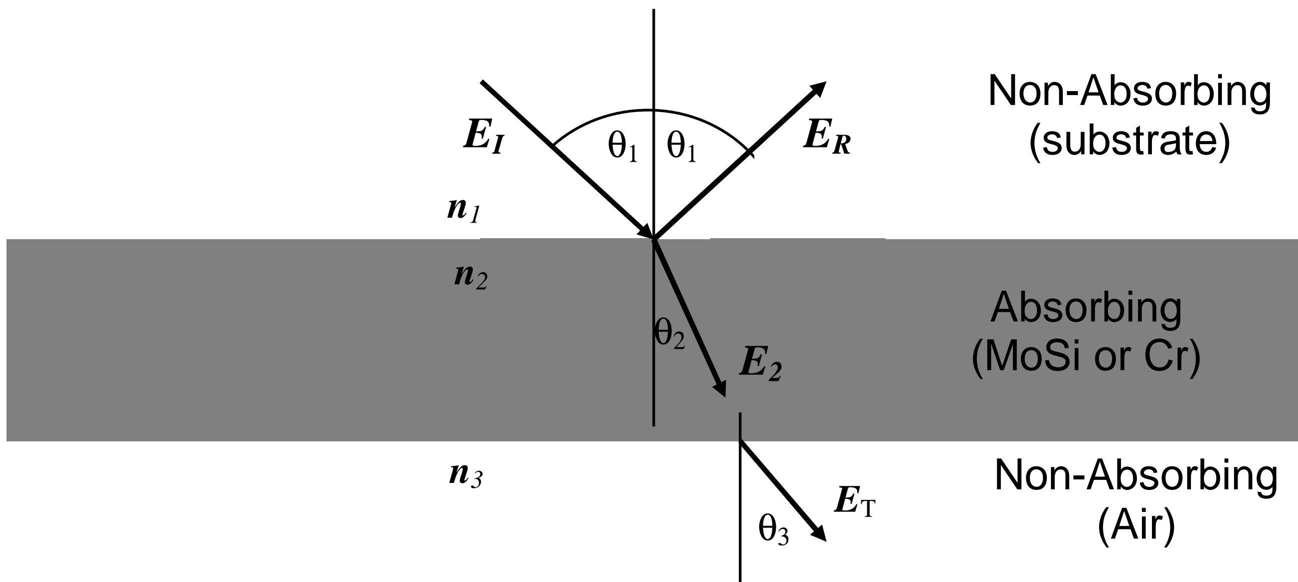

Figure 3: Diagram of a three-layer film stack where the middle layer is absorbing while the top and bottom layers are non-absorbing. The transmissivity for this geometry is calculated as an example problem in Born and Wolf [6]. We apply this as a test for the electric field transmittance of absorber-coated mask blanks.

For this test, we will use the following simulator settings:

Mask Film Stack:

Absorber:	n = 2.343 + 0.586i, 67nm thickness	(typical of a MoSi layer)
Substrate:	n = 1.563117 + 0.0i	(quartz)

Wavelength: 193nm

We choose normally incident illumination for this test problem. For these settings, the transmittance predicted by Born and Wolf is 0.062935, and the amplitude of the incident electric field is 0.819874. This gives a transmitted electric field amplitude of 0.25715. Results were calculated for the two mask topography simulator algorithms available in PROLITH, called EMF1 and EMF2. The speed-accuracy trade-off in PROLITH is controlled by the "Speed Factor". In general, lower Speed Factor numbers correspond to a larger number of grid points so that the results are more accurate, but require more simulation time. Higher Speed Factor settings correspond to coarser grids but require shorter simulation times. The expected trend for a properly functioning simulator is that the errors should become smaller as the Speed Factor setting is decreased.

For EMF1, the errors were all very small, typically less than 10^{-7}. The results for EMF2 are shown in Figure 4. As expected, the errors decrease and the Speed Factor setting is decreased. The impact of these numerical errors on a lithography simulation will be an error in the transmitted intensity of an unpatterned MoSi blank. For EMF1 this error is negligible, and for EMF2, the error in the intensity should be the value in the figure squared, or less than $\sim 10^{-4}$ for most simulator settings. This result demonstrates that the mask topography simulators in PROLITH are providing very accurate results for this test problem.

Downloaded From: http://proceedings.spiedigitallibrary.org/ on 05/06/2014 Terms of Use: http://spiedl.org/terms

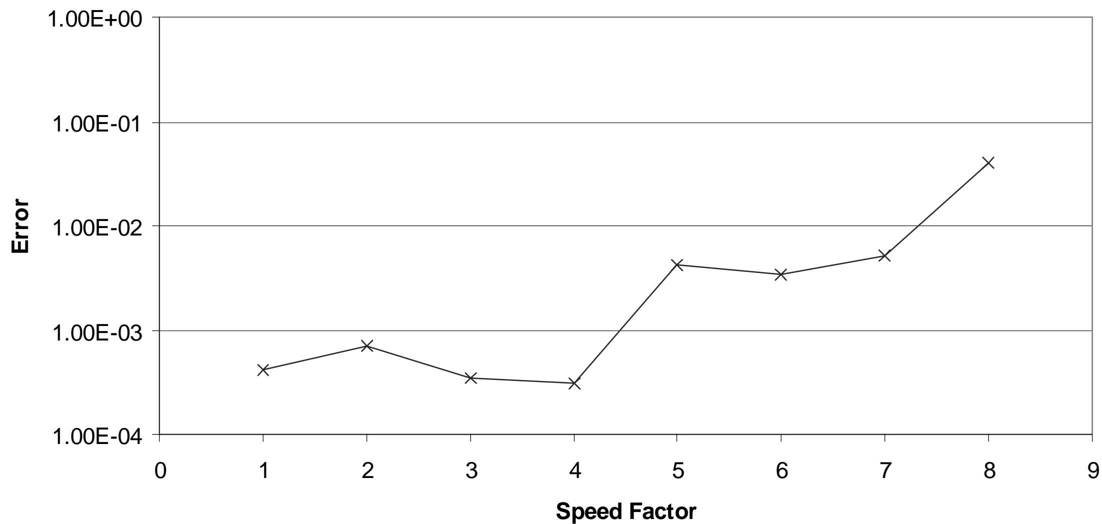

Figure 4: Error in the transmitted electric field amplitude for EMF2 compared with the value calculated in the example in Born and Wolf. The errors for EMF1 are approximately 10^{-8}, so they are not shown on this graph.

4 DIFFRACTION BY A DIELECTRIC GRATING

This benchmark problem follows a method presented by Botten et al. [7], except that here we have adapted the method so that the incident beam passes through the quartz mask blank instead of air. Again, the algebraic details of the solution will not be presented here, but a brief outline of the method is as follows. First, the eigenfunctions for the electric field (S polarization) or for the magnetic field (P polarization) are found inside the grating material. These eigenfunctions can be found analytically but the eigenvalues must be found numerically by solving a transcendental equation. An example eigenfunction is shown in Figure 5. The eigenfunctions represent plane waves propagating in the air and quartz materials which are periodic and continuous across the material interfaces. As shown in the figure, the wavelength of the electric field is larger in the air region than in the quartz region, as expected due to the larger index of refraction for quartz. Because the grating is lossless, the eigenfunctions have the properties that they are self-adjoint, and they form a complete, orthogonal basis for continuous functions [7]. This means that the electric field (or magnetic field) inside the grating can be represented by an infinite series of eigenfunctions.

The electric (or magnetic) fields in the regions above and below the grating are represented by Rayleigh expansions (sets of plane waves). We find the coefficients in the eigenfunction expansion and in the Rayleigh expansions by using the method of moments to enforce the boundary conditions. This leads to a large set of algebraic equations that can be solved using any standard linear algebra package. Of course, the infinite series that is used to represent the fields in the grating and in the regions above and below the grating must be truncated in order to find a numerical solution to the problem. We chose expansions with 21 eigenfunctions and 51 Raleigh modes for the transmitted and reflected fields. Finally, we used Mathematica [8] both to find the eigenvalues and to solve the set of linear algebraic equations.

For this test, we will use the following simulator settings:

Mask Film Stack:
- Substrate: $n = 1.563117 + 0.0i$ (quartz)

Mask pattern: 150nm trenches on a 300nm pitch
Etch depth on the trenches is 170nm

Wavelength: 193nm

Downloaded From: http://proceedings.spiedigitallibrary.org/ on 05/06/2014 Terms of Use: http://spiedl.org/terms

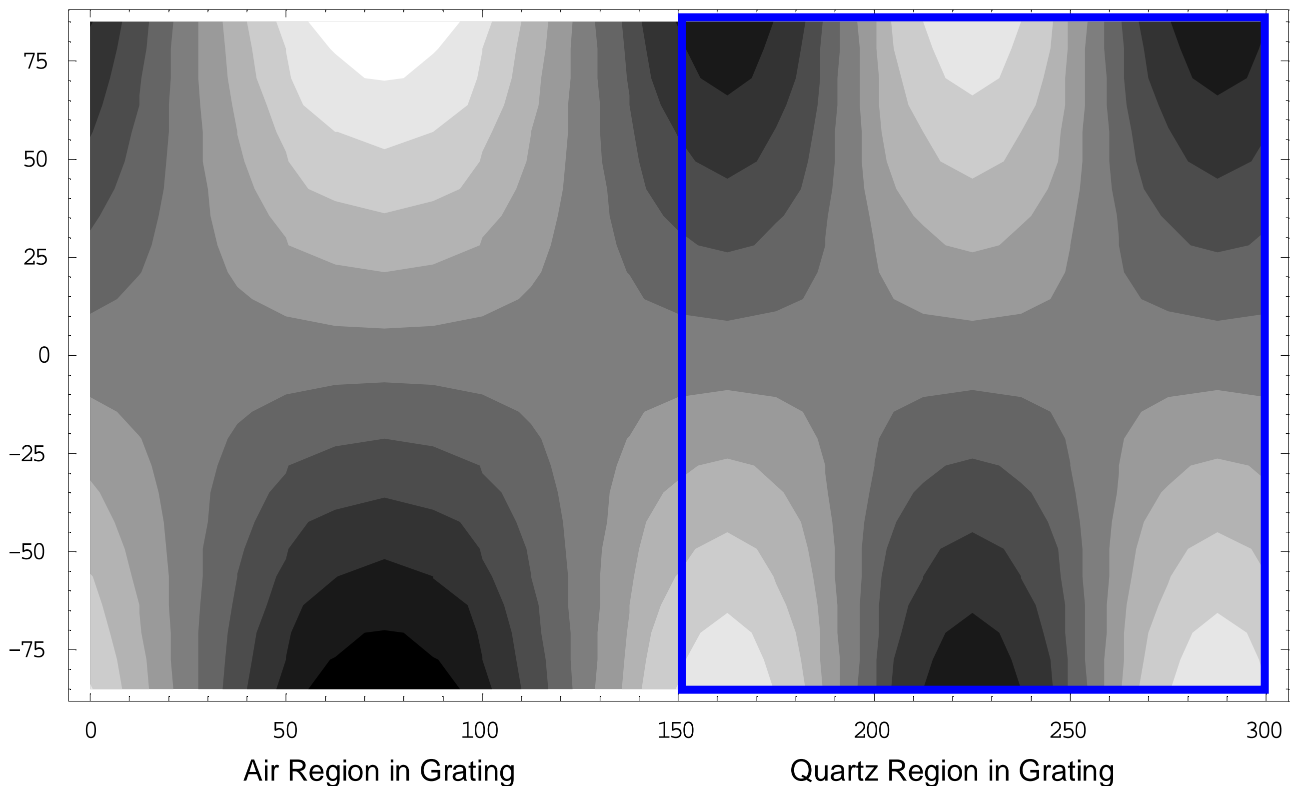

Figure 5: An example eigenfunction for the dielectric grating benchmark problem. The grating in this problem corresponds to a quartz blank with 150nm wide trenches etched 170nm deep.

By using the methods described above, we calculated the amplitude of the electric field for the 0th and the 1st orders in the transmitted diffraction pattern. For s-polarization, the amplitudes were 0.321202 and 0.734797, and for the p-polarization, the amplitudes were 0.326765 and 0.765828. We can calculate the error in the results for the two algorithms in the PROLITH Mask Topography simulator. Results are shown in Figures 6 and 7 for EMF1 and EMF2.

As shown in the figures, the errors become quite small for both EMF1 and EMF2, but it is not immediately obvious how errors in the amplitudes of the diffraction orders will impact downstream results, such as the calculated aerial image or image in resist. It is relatively simple to calculate the expected intensity at the feature edge when using coherent, unpolarized illumination and three-beam imaging. (Three beam imaging will occur when the NA is greater than 193/300 ~ 0.64. Also note that the test problem represents a 1X mask.) The intensity at the wafer will be 1.690984 at the edge of a 75nm feature. We can use this result to calculate errors in the predicted aerial image CD – we use the results used to construct the above figures to calculate an aerial image, and then we extract a CD with an intensity threshold of 1.690984. If the CD is different from 75nm, then this error is caused by the error in the diffraction pattern. Typical errors were less than 0.1nm for EMF1, and less than 1nm for EMF2. This again demonstrates that the simulators are giving reliable, accurate results for this test problem.

Downloaded From: http://proceedings.spiedigitallibrary.org/ on 05/06/2014 Terms of Use: http://spiedl.org/terms

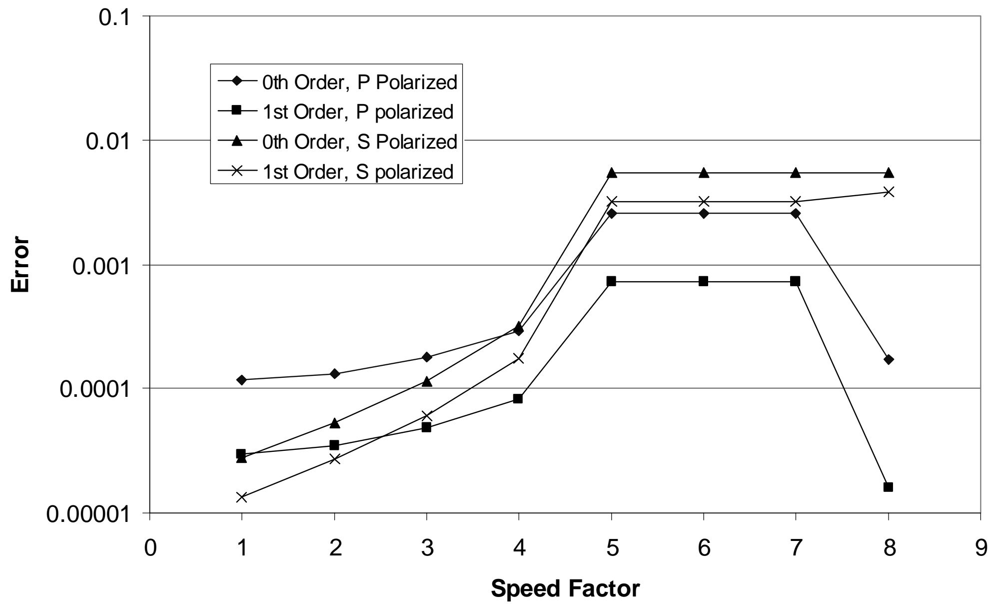

Figure 6: Error in the calculated diffraction pattern for the dielectric grating test problem for EMF1.

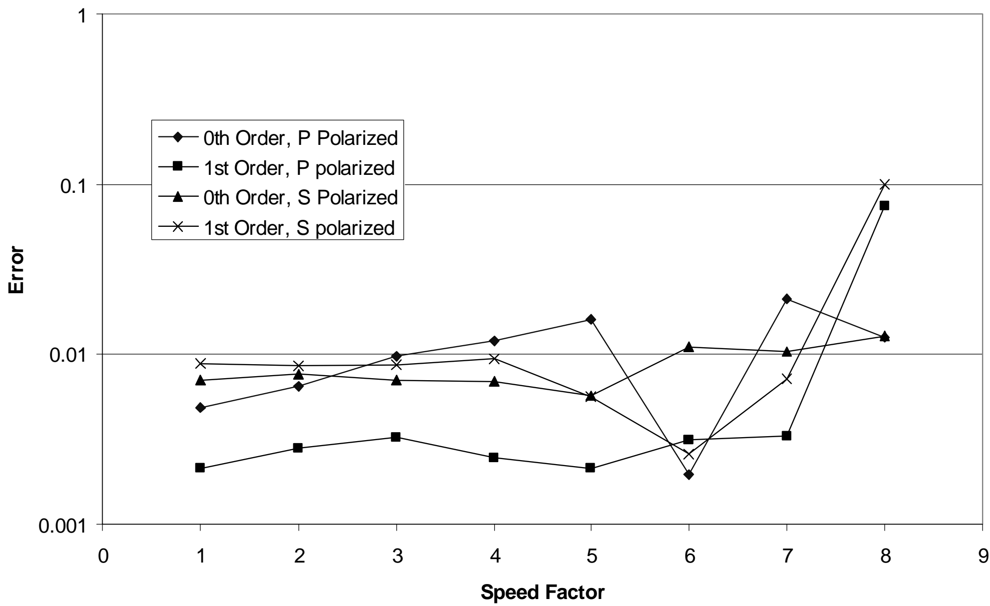

Figure 7: Error in the calculated diffraction pattern for the dielectric grating test problem for EMF2.

Downloaded From: http://proceedings.spiedigitallibrary.org/ on 05/06/2014 Terms of Use: http://spiedl.org/terms

5 SUMMARY AND FUTURE WORK

We have presented two benchmark problems that can be used to quantitatively determine the numerical accuracy of a mask topography simulator based on the rigorous, numerical solution to the Maxwell equations. These problems were chosen so that they were relevant to optical lithography and also so that an absolute accuracy could be calculated. For both problems, PROLITH generated accurate results that were in agreement with the benchmark problems.

For future work, we plan to investigate other grating materials, such as finitely conducting materials, and we also plan to extend these benchmark problems to off-axis illumination and 3D topography, such as square contact holes.

6 REFERENCES

1. ITRS Roadmap, 2000 Update.
2. T. Brunner, “SEMATECH Report: Benchmark tests for image simulation programs used in optical lithography”, SEMATECH (1994)
3. R.L. Gordon, “Exact Computation of 2D Aerial Imagry,” *Proc. SPIE*, Vol. 4692 (2002) pp. 517-528.
4. M.D. Smith, C.A. Mack, “Methods for Benchmarking Photolithography Simulators”, *Proc. SPIE*, Vol. 5040 (2003) pp. 57-68.
5. M.D. Smith, J. D. Byers, C.A. Mack, “Methods for Benchmarking Photolithography Simulators: Part II”, *Proc. SPIE,* Vol. 5377 (2004) pp. 1475-1486.
6. M. Born and E. Wolf, *Principles of Optics*, 6th edition, Pergamon Press (Oxford, 1980).
7. I.C. Botten, M.S. Craig, R.C. McPhedran, J.L. Adams, J.R. Andrewartha, “The dielectric lamellar diffraction grating”, *Optica Acta*, Vol. 28 (1981) pp. 413-428.
8. *Mathematica* version 5.0 is produced by Wolfram Research, Inc., http://www.wolfram.com

Downloaded From: http://proceedings.spiedigitallibrary.org/ on 05/06/2014 Terms of Use: http://spiedl.org/terms